Available online at www.sciencedirect.com
SCIENCE DIRECT
Carbohydrate Research 341 (2006) 433–442
Carbohydrate RESEARCH

Synthesis, structural studies, and cytostatic evaluation of 5,6-di-*O*-modified L-ascorbic acid derivatives

Tatjana Gazivoda,[a] Karlo Wittine,[a] Iva Lovrić,[a] Damjan Makuc,[b] Janez Plavec,[b] Mario Cetina,[c] Draginja Mrvoš-Sermek,[d] Lidija Šuman,[e] Marijeta Kralj,[e] Krešimir Pavelić,[e] Mladen Mintas[a] and Silvana Raić-Malić[a,*]

[a]*Department of Organic Chemistry, Faculty of Chemical Engineering and Technology, University of Zagreb, Marulićev trg 19, HR-10000 Zagreb, Croatia*
[b]*Slovenian NMR Centre, National Institute of Chemistry, Hajdrihova 19, PO Box 660, SL-1001 Ljubljana, Slovenia*
[c]*Faculty of Textile Technology, University of Zagreb, Pierottijeva 6, HR-10000 Zagreb, Croatia*
[d]*Laboratory of General and Inorganic Chemistry, Faculty of Science, University of Zagreb, Zvonimirova 8, HR-10000 Zagreb, Croatia*
[e]*Division of Molecular Medicine, Ruđer Bošković Institute, Bijenička 54, HR-10000 Zagreb, Croatia*

Received 7 November 2005; received in revised form 23 December 2005; accepted 24 December 2005
Available online 24 January 2006

Abstract—The 5,6-di-*O*-tosylated derivative of L-ascorbic acid was synthesized by selective protection and deprotection of 2,3- and 5,6-dihydroxy functional groups involving 5,6-ditosylation in the final step, while the novel 6-acetoxy, 6-hydroxy, and 6-chloro derivatives of 4,5-didehydro-L-ascorbic acid were obtained by reaction of ditosylated compound with nucleophilic reagents. The analysis of $^{3}J_{\text{H-4–H-5}}$ homonuclear coupling constants shows that all L-ascorbic acid derivatives except for epoxy and 4,5-didehydro compounds exist in high population as gauche conformers across C-4–C-5 bonds, while $^{3}J_{\text{C-3–H-5}}$ heteronuclear coupling constants in 4,5-didehydro derivatives indicate cis geometry along C-4–C-5 double bond. The X-ray crystal structure analysis of 2,3-di-*O*-benzyl-5,6-epoxy- and 5,6-isopropylidene-L-ascorbic acid shows that the oxygen atoms attached at positions 2 and 3 of the lactone ring are disposed in a *synperiplanar* fashion. Besides that, the dioxolane ring adopts half-chair conformation. The molecules of epoxy derivative are joined into infinite chains by one weak hydrogen bond of C–H···O type. Two O–H···O, and C–H···O hydrogen bonds link the molecules of 5,6-di-*O*-isopropylidene compound into two-dimensional network. 6-Chloro derivative of 2,3-di-*O*-benzyl-L-ascorbic acid showed the best cytostatic effects against all tested malignant tumor cells (IC_{50}: ~18 μM).

Keywords: L-Ascorbic acid; Configurational analysis; Conformational analysis; Single crystal X-ray diffraction; Cytostatic activity

1. Introduction

L-Ascorbic acid (vitamin C) is the trivial name for the six-carbon sugar derivative L-*threo*-hex-2-enono-1,4-lactone. It is one of the most important biomolecule, which acts as antioxidant and radical scavenger, and is widely distributed in aerobic organisms. Thus, it protects cellular compounds against oxidative damage by free radicals and oxidants.[1] L-Ascorbic acid is present in all foods of plant origin and is an essential micronutrient in man as a consequence of the absence of L-gulonolactone oxidase.[2] It is also crucial for the biosynthesis of collagen, which is a main component of dentin, bone, connective tissue, etc.[3] Furthermore, the biological importance of L-ascorbic acid, known as a putative palliative against the common cold, was initially associated with scurvy, the symptoms of vitamin deficiency.[4] The well-known susceptibility of vitamin C to thermal and oxidative degradation has led to interest in L-ascorbic acid derivatives with increased stability. Numerous simple derivatives of L-ascorbic acid have been synthesized and shown to possess important pharmacological properties. For example, 5,6-di-*O*-modified ascorbic acid

* Corresponding author. Tel.: +385 1 4597 214; fax: +385 1 4597 250; e-mail: silvana.raic@pierre.fkit.hr

0008-6215/$ - see front matter © 2006 Elsevier Ltd. All rights reserved.
doi:10.1016/j.carres.2005.12.010

derivatives were clinically affective antitumor agents for various human cancers[5] and also induced apoptosis in tumor cells,[6] 2-*C*-alkylated derivatives have been shown to have immunostimulant activity,[7] and 2-*O* and 3-*O*-alkylated lipid soluble derivatives are known to protect against the lipid peroxidation of the biomembrane.[8] Some pyrimidine and purine derivatives of 4,5-didehydro-5,6-dideoxy-L-ascorbic acid exerted pronounced cytostatic activities against malignant tumor cell lines.[9]

The present study deals with the synthesis of novel 5,6-di-*O*-modified 4,5-didehydro-L-ascorbic acid derivatives, the configurational and conformational analysis using $^{1}H/^{13}C$ NMR spectroscopy, X-ray crystallography, and the evaluation of their antitumoral potencies.

2. Results and discussion

2.1. Compounds preparation

The 5,6-epoxy **4**[10] and 5,6-di-*O*-acetyl-2,3-di-*O*-benzyl-L-ascorbic acid **8**[10] were synthesized from the starting L-ascorbic acid as outlined in Scheme 1. The 5,6-di-*O*-tosylate derivative of L-ascorbic acid **10** was prepared by a sequence of reactions involving selective protection of 5,6-dihydroxy groups in **7**[11] using toluene-4-sulfonyl chloride. Reaction of the ditosylated compound **10** with sodium acetate gave both, 6-acetoxy **11** and 6-hydroxy **12** derivatives of 4,5-didehydro-L-ascorbic acid. The 6-chloro derivative of 2,3-di-*O*-benzyl-L-ascorbic acid **13** was prepared by reaction of ditosylate **10** with diazobicycloundecane and tetraethylammonium chloride. These reactions of the ditosylated compound **10** most likely involve a two-step reaction pathway in which the first step is an E2 elimination reaction that produces an exocyclic allylic tosylate, which then undergoes an S_N2 reaction with the corresponding nucleophile to give **11** and **13** and in the next step the hydrolysis product **12**. Compounds **11**–**13** were found to exist as *Z*-isomers.

2.2. Configurational and conformational assessment by ^{1}H and ^{13}C NMR

The assignments of ^{1}H and ^{13}C NMR spectra of **2**–**13** are reported in Tables 1 and 2, respectively. *C*-Methyl

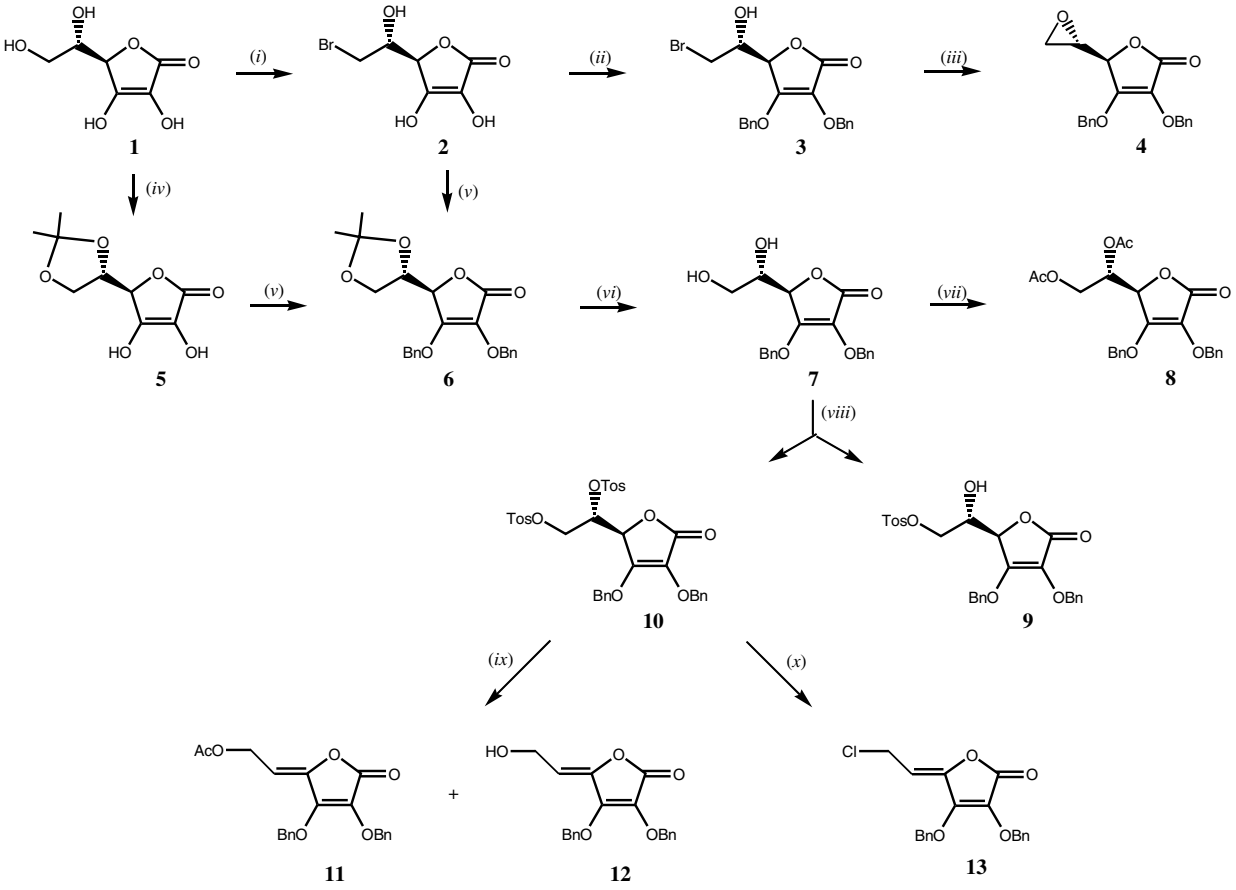

Scheme 1. Reagents: (i) HBr/CH_3COOH; (ii) benzyl chloride, K_2CO_3; (iii) satd aq solution Na_2CO_3; (iv) acetone, acetyl chloride; (v) benzyl chloride, K_2CO_3; (vi) 50% CH_3OOH; (vii) acetic acid anhydride, pyridine; (viii) toluene-4-sulfonyl chloride, pyridine; (ix) NaOAc, DMF; (x) DBU, Et_4NCl.

Table 1. ^{1}H NMR chemical shifts (δ/ppm) and J_{H-H} coupling constants (J/Hz) for compounds **2**–**13**

Compound	Chemical shifts and geminal coupling constants							Vicinal coupling constants	
	CH_3	CH_3^{Tos}	H-6	H-5	H-4	OCH_2	$H^{Ph,Tos}$	$J_{H-4-H-5}$	$J_{H-5-H-6}$
2[a]	—	—	3.51, 3.60; *J* 10.3	4.06	4.92	—	—	2.0	6.8, 6.8
3[c]	—	—	3.51, 3.55; *J* 10.4	4.06	4.87	5.05, 5.10; *J* 11.2 5.18, 5.23; *J* 11.7	7.24–7.41	2.2	6.9, 6.4
4[c]	—	—	2.79, 2.83; *J* 5.0	3.08	4.50	5.06 5.18, 5.23; *J* 11.7	—	4.4	2.7, 4.1
5[b]	1.25	—	3.88, 4.09; *J* 8.3	4.26	4.70	—	—	2.9	6.4, 7.1
6[b]	1.27, 1.29	—	3.88, 4.09; *J* 8.5	4.28	4.96	4.95, 5.02; *J* 11.1 5.17, 5.25; *J* 11.7	7.28–7.42	2.4	6.1, 7.1
7[a]	—	—	3.66	3.87	4.88	5.01 5.17, 5.24; *J* 11.7	7.24–7.43	1.5	6.8
8[c]	1.96, 2.02	—	4.22, 4.29; *J* 11.5	5.33	4.84	5.06, 5.11; *J* 11.2 5.16, 5.22; *J* 11.7	—	2.2	6.8, 5.9
9[c]	—	2.44	4.11, 4.13	4.11	4.65	5.02, 5.07; *J* 11.2 5.16, 5.21; *J* 11.7	7.22–7.80	1.5	2.9, 2.9
10[c]	—	2.41, 2.44	4.08, 4.17; *J* 10.7	5.02	4.77	5.06; *J* 7.1 5.12, 5.25; *J* 11.2	7.28–7.32	1.7	6.6, 6.3
11[b]	2.01	—	4.72	5.46	—	5.15 5.32	7.31–7.43	—	7.1
12[b]	—	—	4.81, 4.81	5.49	—	5.15 5.32	7.31–7.45	—	7.3, 7.3
13[b]	—	—	4.36	5.59	—	5.16 5.33	7.31–7.45	—	8.6

Compounds were dissolved in the following deuterated solvents:
[a] CD_3OD.
[b] Me_2SO-d_6.
[c] $CDCl_3$.

singlets (δ 1.25–1.29) were distinguished from acetyl-methyl (δ 1.96–2.02) and tosyl-methyl (δ 2.41–2.44). In compounds **2**–**10**, proton H-5 is coupled with H-4 (doublet) and H-6 protons (doublet of doublet), which offered their unequivocal assignment. H-5 and H-6 protons were observed at lower field in **11**–**13** in comparison with **2**–**10**. Protons of –OCH_2– (δ 4.95–5.33) and phenyl or tosyl groups (δ 7.22–7.45) were found at similar chemical shifts in all compounds (Table 1).

Analysis of chemical shifts of H-4 in **2**–**10** showed only minor variation with the nature of substituents on the γ-lactone ring with respect to the parent ascorbic acid (Fig. 1). Chemical shift changes of other protons were more pronounced ($\Delta\delta \cong 0.5$–1.5 ppm). H-5 and H-6 protons in **11**–**13** with the exocyclic double bond experience the most downfield chemical shifts. Similar chemical shift changes were observed for acetyl and tosyl groups in **8** and **10**, respectively. The strong impact of oxirane group in **4** was evident from the upfield chemical shifts of H-5 and H-6 protons (Fig. 1).

Spectra gHSQC enabled identification of carbon atoms directly attached to proton resonances that were initially unambiguously assigned. The assignment of quaternary carbon atoms was achieved by gHMBC experiments that showed long-range proton–carbon correlations. Quaternary carbon atoms in 2,2-dimethyl-1,3-dioxolan rings in **5** and **6** (δ 109.06–109.22) are correlated to *C*-methyl protons. C-2 (δ 118.21–123.53) and C═O groups (δ 163.25–173.23) exhibited correlations with H-4 protons, whereas C-3 (δ 163.25–173.23) showed correlations with H-5 protons.

The coupling constants of methylene H-6 protons were resolved in **2**–**6**, **8**, and **10**. Distinct chemical shielding of two H-6 protons in **4**, **5**, and **6** is caused by the nearby 2,2-dimethyl-1,3-dioxolane and oxirane rings (Table 1). $^3J_{H-4-H-5}$ coupling constants were analyzed to assess conformational preference along, C-4–C-5 bond. Generalized Karplus–Altona equation[12] correlates J coupling constants with H–H torsion angles and in addition considers the nature and relative orientation of substituents attached to carbons in the coupled networks. Plots in Figure 2 demonstrate the effect of particular four substituents on C-4 and C-5 carbons on $^3J_{H-4-H-5}$ coupling constant in **2**, **4**, **5**, and **9**. Calculations of $^3J_{H-4-H-5}$ coupling constant as a function of H-4–H-5 torsion angle in other analogues showed very similar curves. Two conformations of H-4–C-4–C-5–H-5 torsion angle were consistent with experimental $^3J_{H-4-H-5}$ coupling constants and were around ±50° and ±105° (Fig. 2). Torsion angle of ±105°, which is a mathematical solution, corresponds to eclipsed conformation that is energetically unfavored.

Although unbiased conformational equilibrium across C-4–C-5 bonds was expected, the analysis of $^3J_{H-4-H-5}$ coupling constants with the use of the generalized Karplus–Altona equation[12] showed that coupling

Table 2. ^{13}C NMR chemical shifts (δ/ppm) for compounds **2–13**

Compound	CH_3	CH_3^{Tos}	C-6	C-5	CH_2	C-4	C-8	C-2	Ph,Tos	Ph (quartC)	Tos (quartC)	C-3	C=O	C=O(Ac)
2[a]	—	—	33.51	70.60	—	77.32	—	120.14	—	—	—	154.36	173.23	—
3[c]	—	—	33.41	70.12	74.24, 74.49	75.83	—	121.71	128.41–129.64	135.98, 136.58	—	157.29	169.45	—
4[c]	—	—	44.22	51.16	74.13, 74.44	75.49	—	121.27	128.25–129.57	136.09, 136.61	—	156.83	169.06	—
5[b]	25.47, 25.86	—	64.90	73.46	—	74.28	109.06	118.21	—	—	—	152.45	170.30	—
6[b]	25.24, 25.68	—	64.81	73.15	72.78, 73.37	74.22	109.22	120.59	127.64–128.79	135.53, 135.98	—	157.35	168.84	—
7[a]	—	—	63.49	70.74	74.76, 75.40	76.92	—	122.44	128.91–130.35	137.33, 137.81	—	159.99	172.33	—
8[c]	20.86, 20.97	—	62.32	68.05	74.25, 74.42	74.21	—	121.96	128.59–129.47	135.88, 136.63	—	155.85	168.95	169.93, 170.70
9[c]	—	21.95	70.23	67.93	74.21, 74.54	75.24	—	121.80	128.41–132.77	135.93, 136.53	132.77, 146.12	156.97	169.55	—
10[c]	—	22.00	66.94	73.25	74.42, 74.92	74.16	—	122.75	128.44–130.55	135.75, 136.68	132.30, 146.40; 133.41, 146.35	154.91	168.46	—
11[c]	20.48	—	57.02	102.74	72.95, 73.92	147.84	—	123.12	127.71–128.60	135.16, 135.65	—	143.01	163.42	170.02
12[b]	—	—	56.44	102.17	72.96, 73.94	147.80	—	123.23	127.64–128.78	135.40, 135.65	—	143.37	163.45	—
13[b]	—	—	36.70	103.90	73.00, 73.97	147.76	—	123.53	127.82–128.75	135.38, 135.64	—	143.42	163.25	—

Compounds were dissolved in the following deuterated solvents:
[a] CD_3OD.
[b] Me_2SO-d_6.
[c] $CDCl_3$.

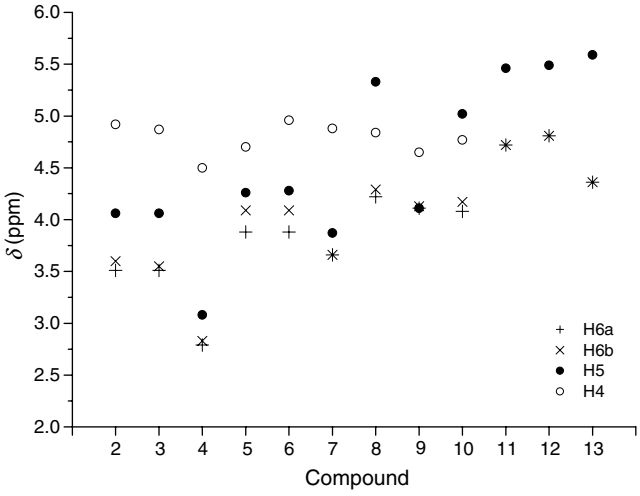

Figure 1. ^{1}H NMR chemical shifts of selected protons in compounds **2–13**.

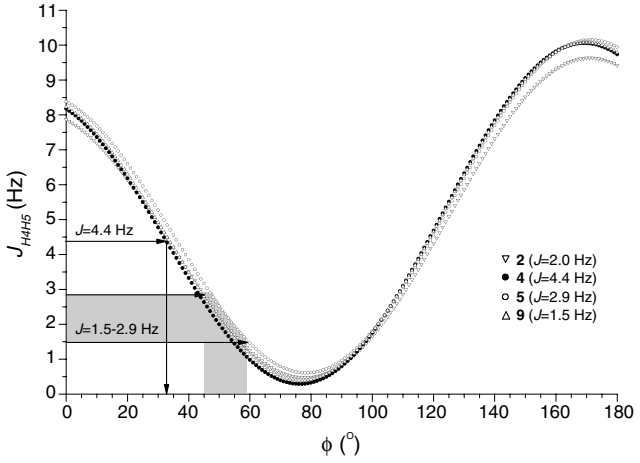

Figure 2. Variation of $^3J_{H\text{-}4\text{–}H\text{-}5}$ coupling constant as a function of H-4–C-4–C-5–H-5 torsion angle. Curves were calculated by the use of Karplus–Altona equation[12] considering the nature and relative orientation of substituents adjacent to coupled protons in **2**, **4**, **5**, and **9**. Experimental coupling constant of 4.4 Hz in **4** corresponds to torsion angle of ca. 33°. The range of experimental coupling constants from 1.5 to 2.9 Hz in **2**, **5**, and **9** as well as other compounds is in agreement with H-4–H-5 torsion angles in the range from 45° to 59°.

constants in the range from 1.5 to 2.9 Hz were in accordance with the high population of gauche conformers across C-4–C-5 bonds in **2**, **3**, and **5**–**10**. Slightly higher $^3J_{H\text{-}4\text{–}H\text{-}5}$ coupling constant in **4** corresponds to smaller torsion angle of ca. ±33°, which reflects conformational constrains imposed by oxirane ring (Fig. 2).

Conformational properties of compounds **2**, **4**, and **6** were evaluated as a function of temperature. ^{1}H NMR spectra were collected at −90, −60, −20, and 20 °C. Coalescence temperature could not be found in this temperature range.

The configuration along C-4–C-5 double bonds in **11**–**13** was evaluated through $J_{C\text{–}H}$ coupling constants.

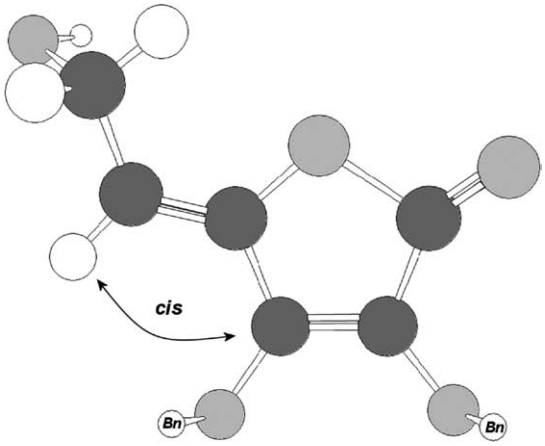

Figure 3. Model of compound **12** with cis configuration along C-4–C-5 double bond as established by long-range $^{3}J_{C\text{-}3\text{–}H\text{-}5}$ coupling constant. For clarity, benzyl groups (Bn) are shown schematically.

Small long-range $^{3}J_{C\text{-}3\text{–}H\text{-}5}$ heteronuclear coupling constants of 5.5, 5.5, and 6.1 Hz in **11**, **12**, and **13**, respectively, are in accordance with cis geometry along C-4–C-5 double bonds[13] (Fig. 3).

2.3. X-ray crystal structure study

2.3.1. Molecular structures. Perspective views of **4** and **5** with their atom-numbering schemes are presented in Figures 4 and 5.

Compound **4** consists of a planar lactone ring with two benzyloxy groups attached to the ring atoms C-2 and C-3, and an epoxypropyl moiety attached to the C-4 atom (Fig. 4). The bond lengths in the lactone ring

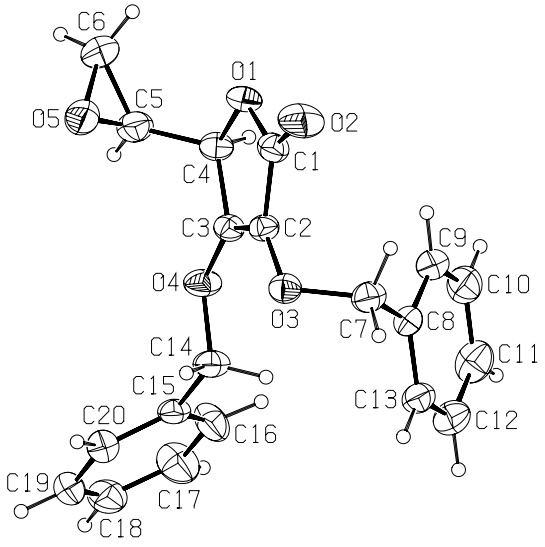

Figure 4. A view of **4** with the atom-numbering scheme. Displacement ellipsoids for non-hydrogen atoms are drawn at the 30% probability level and hydrogen atoms are drawn as small circles of arbitrary radii.

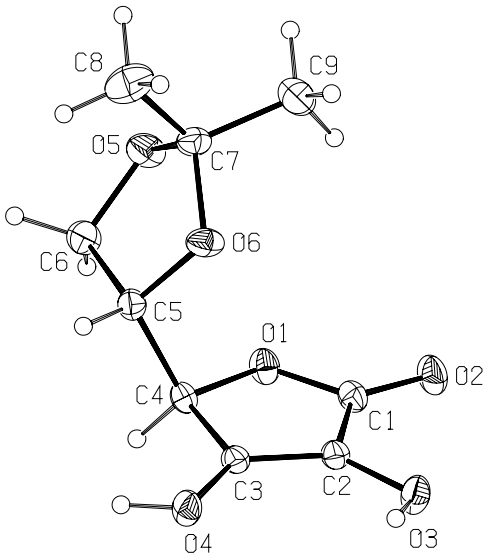

Figure 5. A view of **5** with the atom-numbering scheme. Displacement ellipsoids for non-hydrogen atoms are drawn at the 30% probability level and hydrogen atoms are drawn as small circles of arbitrary radii.

and benzyloxy groups are within the values found in structurally related 2,3-di-*O*-benzyl ethers of L-ascorbic acid.[14] In **5**, two hydroxyl groups are attached to the C-2 and C-3 atoms and a dioxolane ring to the C-4 atom of the lactone ring (Fig. 5). The bond lengths in the lactone and dioxolane rings agree well with the equivalent ones in 5,6-di-*O*-isopropylidene-L-ascorbic acid derivatives.[14,15]

The oxygen atoms O-3 and O-4 are disposed in a *syn-periplanar* fashion in both structures; the O-3–C-2–C-3–O-4 torsion angle amounts to −0.7(8)° and 1.0(3)° in **4** and **5**, respectively. The conformation of **4** could also be described by torsion angles in which the atoms of the lactone and other rings are included: C-2–O-3–C-7–C-8 [−67.3(4)°], C-3–O-4–C-14–C-15 [177.5(4)°], C-3–C-4–C-5–O-5 [73.2(5)°], and C-3–C-4–C-5–C-6 [144.0(5)°]. The dihedral angle between the epoxypropyl ring and the mean plane of the lactone ring is 64.9(5)°. The orientation of the phenyl C-15–C-20 ring in **4** with respect to the lactone ring differs slightly compared with the orientation of the C-8–C-13 ring. The dihedral angles between the mean planes of the C-15–C-20 and C-8–C-13 rings and the lactone ring are 76.7(3)° and 50.8(2)°. The dioxolane ring in **5** adopts half-chair conformation, twisted around the C-7–O-5 bond.

2.3.2. Crystal structures. The molecules of **4** are linked by only one weak hydrogen bond of C–H···O type (Fig. 6 and Table 3). Atom C-9 in **4** acts as a donor to O-2 atom, hence generating a $C(8)$ chain motif[16] parallel to the *a* axis and generated by the 2_1 axis.

In **5**, the O-3···O-5 hydrogen bond joins the molecules parallel to the *b* axis, thus forming $C(8)$ chain

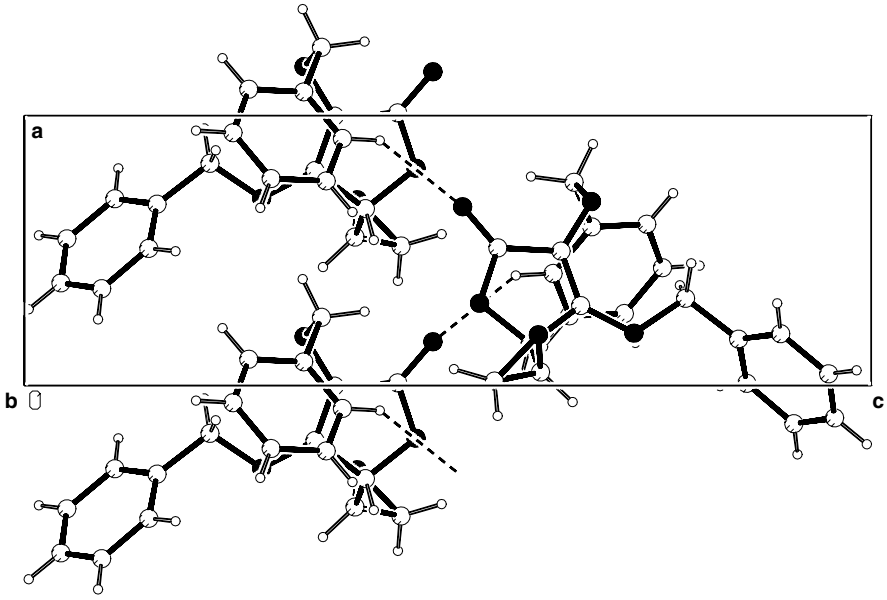

Figure 6. A crystal packing diagram of **4**, viewed along the *b* axis, showing a *C*(8) chain motif formed by only one (C-9···O-2) hydrogen bond. Hydrogen bonds are indicated by dashed lines.

Table 3. Hydrogen-bonding geometry for **4** and **5**

	D–H···A	D–H (Å)	H···A (Å)	D···A (Å)	D–H···A (°)	Symmetry codes
4	C-9–H-9···O-2	0.93	2.45	3.256(6)	145	$-1/2+x$, $1/2-y$, $1-z$
5	O-3–H-3···O-5	0.85(2)	1.87(2)	2.711(2)	170(3)	x, $-1+y$, z
	O-4–H-4···O-2	0.90(3)	1.81(3)	2.706(2)	172(3)	$1+x$, y, z
	C-5–H-5···O-2	0.94(2)	2.46(2)	3.124(2)	128(2)	$1+x$, y, z
	C-9–H-9···O-6	0.96	2.60	3.494(3)	155	$1-x$, $1/2+y$, $3/2-z$

motif generated by translation (Fig. 7 and Table 3). The molecules are also linked by O-4···O-2 hydrogen bond, hence producing *C*(6) chain motif generated by translation and parallel to the *a* axis. The combination of these two chain motifs forms $R_4^4(25)$ rings (Fig. 7) and leads to a (4,4) net.[17] The action of these hydrogen bonds is reinforced by that of the two C–H···O hydrogen bonds. The C-5···O-2 hydrogen bond links the molecules parallel to the *a* axis, hence forming *C*(6) chain motif generated by translation (Fig. 7). The O-2 atom is a bifurcated acceptor, and O-4···O-2 and C-5···O-2 hydrogen bonds thus generate $R_2^1(7)$ chain of rings. In addition, C-9 atom acts as a donor to O-6 atom of the neighboring molecule, so forming *C*(4) chain motif parallel to the *b* axis and generated by the 2_1 screw axis. The C-9···O-6 hydrogen bond links (4,4) nets into two-dimensional network (Fig. 7).

2.4. Cytostatic activity

Compounds **1**–**10**, **12**, and **13** were evaluated for their cytostatic activities against malignant human tumor cell lines: cervical carcinoma (HeLa), breast carcinoma (MCF-7), pancreatic carcinoma (MiaPaCa-2), laryngeal carcinoma (Hep-2), and colon carcinoma (SW 620), as well as human fibroblast cells (WI 38) (Table 4).

L-Ascorbic acid itself did not exhibit antitumor activity against all tumor and normal cell lines in tested concentrations, except for low cytostatic effect against colon carcinoma (IC_{50} >100 μM). Compounds containing free hydroxy groups attached at positions 2 and 3 of the lactone ring (**2** and **5**), and two hydroxy groups at positions 5 and 6 in the side chain **7**, as well as 5,6-di-*O*-isopropylidene derivative of L-ascorbic acid **6** did not show inhibitory effect on examined tumor cell lines. On the contrary to this, 2,3-di-*O*-benzylated derivatives of L-ascorbic acid (**3**, **4**, **8**–**10**, **12**, and **13**) showed rather marked antitumor activity against all evaluated cell lines with IC_{50} in the range of 17–79 μM (Table 4). 6-Hydroxy **12** and 6-chloro **13** derivatives of L-ascorbic acid exhibited the best cytostatic effects against all malignant tumor cells (Fig. 8). Besides, **12** showed the best selectivity, since it inhibited the growth of tumor, but not of normal cells.

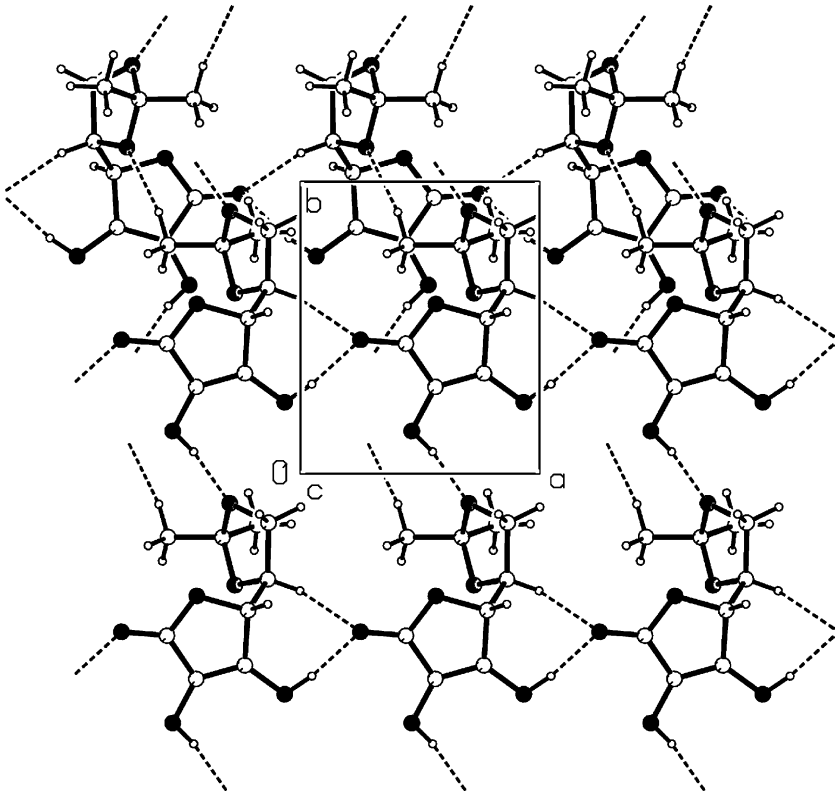

Figure 7. A crystal packing diagram of **5**, viewed along the *c* axis, showing the O-3···O-5, O-4···O-2, C-5···O-2, and C-9···O-6 hydrogen bonds. The O-3···O-5 and O-4···O-2 hydrogen bonds generate a (4,4) net of $R_4^4(25)$ rings, while the O-4···O-2 and C-5···O-2 hydrogen bonds form $R_2^1(7)$ chain of rings. The C-9···O-6 hydrogen bond links (4,4) nets into two-dimensional network. Hydrogen bonds are indicated by dashed lines.

Table 4. Inhibitory effects of L-ascorbic acid derivatives on the growth of malignant tumor cell lines and diploid fibroblasts (WI 38)

Compound	Tumor cell growth [IC_{50}[a] (μM)]					
	HeLa	MCF-7	MiaPaCa-2	Hep-2	SW 620	WI 38
1	>100	>100	>100	>100	>100	>100
2	>100	>100	>100	>100	>100	>100
3	20 ± 6	27 ± 21	19 ± 1	34 ± 20	18 ± 3	55 ± 13
4	22 ± 9	26 ± 13	17 ± 1	31 ± 12	20 ± 2	58 ± 8
5	>100	>100	>100	>100	>100	>100
6	>100	>100	>100	>100	⩾100	>100
7	>100	>100	>100	>100	>100	>100
8	16 ± 2	28 ± 4	21 ± 4	20 ± 2	38 ± 30	15 ± 3
9	16 ± 3	21 ± 6	18 ± 0.7	31 ± 30	28 ± 12	22 ± 4
10	26 ± 18	30 ± 9	20 ± 13	59 ± 20	⩾100	18 ± 4
12	19.3 ± 0.2	29 ± 9	23 ± 7	21 ± 7	27 ± 4	>100
13	17 ± 6	17 ± 0.4	18 ± 0.4	17 ± 2	19 ± 0.2	26 ± 1

[a] 50% inhibitory concentration, or compound concentration required to inhibit tumor cell proliferation by 50%.

3. Conclusions

The 5,6-di-*O*-tosylated derivative of 2,3-di-*O*-benzyl-L-ascorbic acid **10** was synthesized by using the strategy of selective protection and deprotection of 2,3- and 5,6-dihydroxy functional groups and subsequent tosylation of 5,6-dihydroxy groups. Reactions of **10** with appropriate nucleophiles gave novel 6-acetoxy **11**, 6-hydroxy **12**, and 6-chloro **13** derivatives of 4,5-didehydro-L-ascorbic acid existing as *Z*-isomers. The analysis of $^3J_{H\text{-}4\text{–}H\text{-}5}$ coupling constants shows that coupling constants in the range from 1.5 to 2.9 Hz are in accordance with high population of gauche conformers across C-4–C-5 bonds in **2**, **3**, and **5**–**10**. Small long-range $^3J_{C\text{-}3\text{–}H\text{-}5}$ heteronuclear coupling constants of 5.5, 5.5, and 6.1 Hz in **11**, **12**, and **13**, respectively, indicate cis geometry along the C-4–C-5 double bond. The exact stereostructures of 5,6-di-*O*-isopropylidene-L-ascorbic acids **4** and

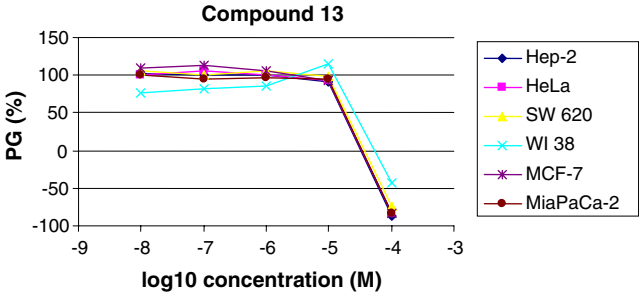

Figure 8. Dose–response profile for compound **13** tested in vitro (PG = percentage of growth).

2,3-di-*O*-benzyl-5,6-epoxy-L-ascorbic acid **5** were unambiguously determined by X-ray crystal structure analysis. Among all compounds evaluated for their cytostatic activities, the 6-chloro derivatives of 2,3-di-*O*-benzyl-L-ascorbic acid **13** showed the best cytostatic effects against all malignant tumor cells (IC_{50}: ~18 μM).

4. Experimental

4.1. General methods

Melting points (uncorrected) were determined with Kofler micro hot-stage (Reichert, Wien). Precoated E. Merck Silica Gel 60F-254 plates were used for thin layer chromatography (TLC) and the spots were detected under UV light (254 nm). Column chromatography (CLC) was performed using silica gel (0.063–0.2 mm) Kemika; glass column was slurry-packed under gravity. The electron impact mass spectra were recorded with an EXTREL FT MS 2001 instrument with an ionizing energy of 70 eV.

4.2. Compounds preparation

6-Bromo-L-ascorbic acid **2**,[18] 6-bromo-2,3-di-*O*-benzyl-L-ascorbic acid **3**,[19] 2,3-di-*O*-benzyl-4-(5,6)-epoxy-L-ascorbic acid **4**,[10] 5,6-di-*O*-isopropylidene-L-ascorbic acid **5**,[11] 2,3-di-*O*-benzyl-5,6-*O*,*O*-isopropylidene-L-ascorbic acid **6**,[11] 2,3-di-*O*-benzyl-L-ascorbic acid **7**,[11] 5,6-di-*O*-acetyl-2,3-di-*O*-benzyl-L-ascorbic acid **8**,[10] and 2,3-di-*O*-benzyl-6-*O*-tosyl-L-ascorbic acid **9**[19] were synthesized in accord with original procedures given in the literature.

4.2.1. 2,3-Di-*O*-benzyl-5,6-di-*O*-tosyl-4,5-didehydro-L-ascorbic acid 10. Reaction mixture of 2,3-di-*O*-benzyl-L-ascorbic acid **7** (17.8 g, 0.05 mol), anhyd pyridine (50 mL), and CH_2Cl_2 (150 mL) was stirred at 0 °C under argon. Toluene-4-sulfonyl chloride (21 g, 0.11 mol) dissolved in anhyd CH_2Cl_2 (100 mL) was added dropwise to this solution. The stirring of the reaction mixture was continued at room temperature for 24 h. When the reaction was completed, solution was diluted with CH_2Cl_2 (400 mL), then washed twice with water and dried over Na_2SO_4. Solvent was evaporated and the crude product was recrystallized from EtOH to give colorless crystals of **10** ($m = 22.6$ g, mp = 105–106 °C, 70%); EIMS *m*/*z* 665 ($M^{+\cdot}$). Anal. Calcd for $C_{34}H_{32}O_{10}S_2$: C, 61.43; H, 4.85. Found: C, 61.51; H, 4.86.

4.2.2. *Z*-6-*O*-Acetyl-2,3-di-*O*-benzyl-4,5-didehydro-L-ascorbic acid 11 and *Z*-2,3-di-*O*-benzyl-6-hydroxy-4,5-didehydro-L-ascorbic acid 12. To a solution of ditosylate **10** (4 g, 6 mmol) in dry DMF (110 mL), NaOAc (972 mg, 18 mmol) was added and the resulting mixture was stirred at 50–60 °C under nitrogen for 5 h. The solvent was evaporated and Et_2O (20 mL) was added, followed by H_2O (20 mL). The organic layer was separated and washed further with H_2O (2 × 20 mL) before being dried over $MgSO_4$. Filtration and evaporation of the solvent gave a yellow oil, which was purified by column chromatography (40:1 CH_2Cl_2–MeOH) to give pure oily compounds **11** (423 mg, 19%) and **12** (586 mg, 29%). Compound **11**, EIMS *m*/*z* 380 ($M^{+\cdot}$). Anal. Calcd for $C_{22}H_{20}O_6$: C, 69.46; H, 5.30. Found: C, 69.32; H, 5.31. Compound **12**, EIMS *m*/*z* 338 ($M^{+\cdot}$). Anal. Calcd for $C_{20}H_{18}O_5$: C, 70.99; H, 5.36. Found: C, 71.11; H, 5.37.

4.2.3. *Z*-2,3-Di-*O*-benzyl-6-chloro-4,5-didehydro-L-ascorbic acid 13. A mixture of the ditosylate **10** (1 g, 1.5 mmol), in MeCN (15 mL), diazobicycloundecane (DBU, 230 mg, 1.5 mmol), and Et_4NCl (250 mg, 1.5 mmol) was refluxed for 16 h. The solvent was evaporated and CH_2Cl_2 (20 mL) was added, followed by water (20 mL). The organic layer was separated and dried over $MgSO_4$. Filtration and evaporation of the solvent gave a residue, which was purified by column chromatography (30:1 CH_2C_2–MeOH) affording **13** (217 mg, 41%) as a brown oil; ESMS *m*/*z* 356 ($M^{+\cdot}$). Anal. Calcd for $C_{20}H_{17}ClO_4$: C, 67.32; H, 4.80. Found: C, 67.11; H, 4.79.

4.3. NMR Measurements

^1H and ^{13}C NMR spectra were collected on Varian Unity Inova 300 MHz NMR spectrometer equipped with 5 mm $^1H\{^{15}N–^{31}P\}$ indirect-detection probe with gradients. All data were recorded at 25 °C unless specified otherwise. Proton and carbon chemical shifts were referenced relative to the solvent signal of Me_2SO-d_6 (**5**, **6**, **11**, **12**, and **13**), CD_3OD (**2** and **7**) or CD_2Cl_2 (**3**, **4**, **8**, **9**, and **10**). Individual resonances were assigned on the basis of their chemical shifts, signal intensities, magnitude, and multiplicity of resonances, H–H and C–H coupling constants involved as well as with the use of a series of 2D experiments.

The pulse sequences of gHSQC and gHMBC experiments were taken from Varian software library. The gHSQC spectra were used for single-bond $^{1}H–^{13}C$ chemical shift correlations and utilized BIRD sequence and GARP ^{13}C decoupling. Two sets of 128 time increments were acquired with 32 scans per increment and 2.5 s relaxation delay. The data were zero filled and processed with Gaussian weighting functions. The gHMBC spectra were used to assign multiple-bond $^{1}H–^{13}C$ chemical shift correlations with delays set according to anticipated long-range coupling constant of 8 Hz. Data were collected with 64 scans using 128 increments and a relaxation delay of 2.5 s, then zero filled and processed with squared shifted sine-bell weighting functions.

Cis and trans configurations along C-4–C-5 double bonds in **11**, **12**, and **13** were deduced from heteronuclear vicinal $J_{C–H}$ coupling constants obtained by INEPT sequence. Experiment was optimized for C–H coupling constant of 20 Hz with relaxation delay of 2.0 s.

4.4. X-ray crystal structure study

The single crystals of **4** and **5** were obtained at room temperature by slow evaporation of an EtOH soln (96%). The intensities were collected at 293 K on Oxford Diffraction Xcalibur 2 diffractometer with graphite-monochromated Mo K_α radiation. The data collection and reduction were carried out with the CrysAlis programs.[20] Details of crystal data, data collection, and refinement parameters are given in Table 5.

The crystal structures were solved by direct methods. All non-hydrogen atoms were refined anisotropically by full-matrix least-squares calculations based on F^2. All hydrogen atoms in **4** and hydrogen atoms attached to the C-8 and C-9 atoms in **5** were treated using appropriate riding models. All other hydrogen atoms in **5** were found in a difference Fourier map and their coordinates and isotropic thermal parameters were refined freely. Programs used for structure solution, refinement, and analysis include SHELXS97,[21] SHELXL97,[22] and PLATON.[23] The molecular and crystal structure drawings were prepared by PLATON program.[23]

4.5. Cytostatic activity assays

The experiments were carried out on six human cell lines, five of which are derived from five cancer types and one normal, fibroblast cell line. The following cell lines were used: HeLa (cervical carcinoma), MCF-7 (breast carcinoma), MiaPaCa-2 (pancreatic carcinoma), Hep-2 (laryngeal carcinoma), SW 620 (colon carcinoma), and WI 38 (diploid fibroblasts).

The cells were cultured as monolayers and maintained in Dulbecco's Modified Eagle Medium (DMEM) supplemented with 10% fetal bovine serum (FBS), 2 mM L-glutamine, 100 U/mL penicillin, and 100 μg/mL streptomycin in a humidified atmosphere with 5% CO_2 at 37 °C.

The panel cell lines were inoculated onto a series of standard 96-well microtiter plates on day 0 at 1×10^4–3×10^4 cells/mL, depending on the doubling times of specific cell line. Test agents were then added in five, 10-fold dilutions (10^{-8}–10^{-4} M) and incubated for further 72 h. Working dilutions were freshly prepared on the day of testing. The compounds were prepared as 0.1 M solns in Me_2SO, and the solvent was also tested for eventual inhibitory activity by adjusting its concentration to be the same as in working concentrations. After 72 h of incubation the cell growth rate was evaluated by performing the MTT assay (Sigma),[24] which detects dehydrogenase activity in viable cells. The MTT Cell Proliferation Assay is a colorimetric assay system, which measures the reduction of a tetrazolium component (MTT) into an insoluble formazan product by the mitochondria of viable cells. For this purpose the substance treated medium was discarded and MTT was

Table 5. Crystal data and summary of data collection and refinement for **4** and **5**

Compound	**4**	**5**
Formula	$C_{20}H_{18}O_5$	$C_9H_{12}O_6$
Formula weight	338.34	216.19
Temperature [K]	293(2)	293(2)
Radiation [Å]	0.71073	0.71073
Crystal size [mm]	$0.45 \times 0.20 \times 0.10$	$0.60 \times 0.56 \times 0.25$
Crystal color, shape	Colorless, prismatic	
Crystal system, space group	Orthorhombic, $P2_12_12_1$ (No. 19)	
Unit cell dimensions		
a [Å]	6.028(2)	6.3838(10)
b [Å]	15.272(3)	7.7898(9)
c [Å]	18.907(3)	19.774(2)
V [Å^3]	1740.6(7)	983.3(2)
Z	4	4
D_{calcd} [g cm^{-3}]	1.291	1.460
Absorption coefficient μ [mm^{-1}]	0.093	0.124
F(0 0 0)	712	456
Scan-mode	ω and φ	ω
θ range for data collection [°]	4.44–21.99	4.13–30.00
Index ranges	$-6 \leqslant h \leqslant 6$ $-16 \leqslant k \leqslant 16$ $-19 \leqslant l \leqslant 19$	$-4 \leqslant h \leqslant 8$ $-10 \leqslant k \leqslant 9$ $-27 \leqslant l \leqslant 27$
Collected reflections	16479	7031
Independent reflections/$R_{int.}$	2121/0.1111	2732/0.0290
Reflection number $I \geqslant 2\sigma(I)$	1873	2524
Data/restraints/parameters	2121/0/229	2732/0/162
Weighting parameters a, b[a]	0.0505, 0.8970	0.0442, 0.3803
Goodness-of-fit on F^2	1.056	0.992
$R[I \geqslant 2\sigma(I)]$	0.0643	0.0418
$wR[I \geqslant 2\sigma(I)]$	0.1208	0.0976
Max./min. electron density [e Å^{-3}]	0.112/−0.130	0.224/−0.190

[a] $w = 1/[\sigma^2(F_o^2) + (aP)^2 + bP]$, where $P = (F_o^2 + 2F_c^2)/3$.

added to each well at a concentration of 20 μg/40 μL. After 4 h of incubation the precipitates were dissolved in 160 μL of Me_2SO. The absorbency (OD, optical density) was measured on a microplate reader at 570 nm. The absorbency is directly proportional to the cell viability. The percentage of growth (PG) of the cell lines was calculated according to one or the other of the following two expressions:

If $(\text{mean OD}_{\text{test}} - \text{mean OD}_{\text{tzero}}) \geqslant 0$ then

$$\text{PG} = 100 \times (\text{mean OD}_{\text{test}} - \text{mean OD}_{\text{tzero}})/(\text{mean OD}_{\text{ctrl}} - \text{mean OD}_{\text{tzero}}).$$

If $(\text{mean OD}_{\text{test}} - \text{mean OD}_{\text{tzero}}) < 0$ then

$$\text{PG} = 100 \times (\text{mean OD}_{\text{test}} - \text{mean OD}_{\text{tzero}})/\text{OD}_{\text{tzero}},$$

where mean OD_{tzero} = the average of optical density measurements before exposure of cells to the test compound; mean OD_{test} = the average of optical density measurements after the desired period of time; mean OD_{ctrl} = the average of optical density measurements after the desired period of time with no exposure of cells to the test compound.

Each test point was performed in quadruplicate in three individual experiments. The results were expressed as IC_{50}, a concentration necessary for 50% of inhibition. Each result is a mean value from three separate experiments.

5. Supplementary data

CCDC 274566 (**4**) and 274567 (**5**) contain the supplementary crystallographic data for this paper. These data can be obtained free of charge via www.ccdc.cam.ac.uk/data_request/cif, by emailing data_request@ccdc.cam.ac.uk, or by contacting The Cambridge Crystallographic Data Centre, 12, Union Road, Cambridge CB2 1EZ, UK; fax: +44 1223 336033.

Acknowledgments

Support for this study was provided by the Ministry of Science of the Republic of Croatia (Projects #0125003 and #00981499).

References

1. Wimalasena, K.; Mahindaratne, M. P. D. *J. Org. Chem.* **1994**, *59*, 3427–3432.
2. Nath, M.; Jairath, R.; Eng, G.; Song, X.; Kumar, A. *Spectrochim. Acta, Part A* **2005**, *61*, 77–86.
3. Sakamoto, Y.; Takano, Y. *Tissue Cell* **2005**, *37*, 11–23.
4. Ge, P.; Kirk, K. L. *J. Org. Chem.* **1997**, *62*, 3340–3343.
5. (a) Kochi, M.; Takeuchi, S.; Mitzutani, T.; Mochizuki, K.; Matsumoto, Y.; Saito, Y. *Cancer Treat Rep.* **1980**, *64*, 21–23; (b) Kochi, M.; Isono, N.; Niwayama, M.; Shirakabe, K. *Cancer Treat Rep.* **1985**, *69*, 533–537; (c) Kochi, M.; Ueda, S.; Tagiwara, T. *Progr. Cancer Res. Ther.* **1988**, *35*, 338–343; (d) Sakagami, H.; Asano, K.; Fukuchi, K.; Gomi, K.; Ota, H.; Kazama, K.; Tanuma, S.; Kochi, M. *Anticancer Res.* **1991**, *11*, 1533–1540.
6. Tanuma, S.; Shiokawa, D.; Tanimoto, Y.; Ikekita, M.; Sakagami, H.; Takeda, M.; Fukuda, S.; Kochi, M. *Biochem. Biophys. Res. Commun.* **1993**, *194*, 29–35.
7. (a) Veltri, R. W.; Fodor, G.; Liu, C. M.; Woolverton, C. J.; Baseler, M. W. *J. Biol. Res. Mod.* **1986**, *5*, 444–461; (b) Woolverton, C. J.; Veltri, R. W.; Snyder, I. S. *J. Biol. Res. Mod.* **1986**, *5*, 527–538.
8. Nihro, Y.; Miyataka, H.; Sudo, T.; Matsumoto, H.; Satoh, T. J. *J. Med. Chem.* **1991**, *34*, 2152–2157.
9. (a) Raić-Malić, S.; Hergold-Brundić, A.; Nagl, A.; Grdiša, M.; Pavelić, K.; De Clercq, E.; Mintas, M. *J. Med. Chem.* **1999**, *42*, 2673–2678; (b) Gazivoda, T.; Plevnik, M.; Plavec, J.; Kraljević, S.; Kralj, M.; Pavelić, K.; Balzarini, J.; De Clercq, E.; Mintas, M.; Raić-Malić, S. *Bioorg. Med. Chem.* **2005**, *13*, 131–139.
10. Raić-Malić, S.; Svedružić, D.; Gazivoda, T.; Marunović, A.; Hergold-Brundić, A.; Nagl, A.; Balzarini, J.; De Clercq, E.; Mintas, M. *J. Med. Chem.* **2000**, *43*, 4806–4811.
11. Dallacker, V. F.; Sanders, J. *Chem. Ztg.* **1985**, *109*, 197–202.
12. Altona, C.; Ippel, J. H.; Westra Hoekzema, A. J. A.; Erkelens, C.; Groesbeek, M.; Donders, L. A. *Magn. Reson. Chem.* **1989**, *27*, 564–576.
13. Hocková, D.; Buděšínský, M.; Marek, R.; Marek, J.; Holý, A. *Eur. J. Org. Chem.* **1999**, *10*, 2675–2682.
14. Wittine, K.; Gazivoda, T.; Markuš, M.; Mrvoš-Sermek, D.; Hergold-Brundić, A.; Cetina, M.; Žiher, D.; Gabelica, V.; Mintas, M.; Raić-Malić, S. *J. Mol. Struct.* **2004**, *687*, 101–106.
15. Ries, A.; Sander, J.; Hegetschweiler, K. *Z. Kristallogr.—New Cryst. Struct.* **2001**, *216*, 577–578.
16. Bernstein, J.; Davis, R. E.; Shimoni, L.; Chang, N.-L. *Angew. Chem., Int. Ed. Engl.* **1995**, *34*, 1555–1573.
17. Batten, S. R.; Robson, R. *Angew. Chem., Int. Ed.* **1998**, *37*, 1460–1494.
18. Osmak, M.; Eckert-Maksić, M.; Pavelić, K.; Maksić, Z. B.; Spaventi, R.; Beketić, L.; Kovaček, I.; Šušković, B. *Res. Exp. Med.* **1990**, *190*, 443–449.
19. Dallacker, V. F.; Sanders, J. *Chem. Ztg.* **1985**, *109*, 277–280.
20. Oxford Diffraction, Xcalibur CCD System. CrysAlis CCD and CrysAlis RED. Versions 1.4. Oxford Diffraction, Oxford, United Kingdom, 2004.
21. Sheldrick, G. M. SHELXS97, Program for the Solution of Crystal Structures. University of Göttingen, Germany, 1997.
22. Sheldrick, G. M. SHELXL97, Program for the Refinement of Crystal Structures. University of Göttingen, Germany, 1997.
23. Spek, A. L. PLATON, A Multipurpose Crystallographic Tool. Utrecht University, The Netherlands, 2002.
24. Mossman, T. *J. Immunol. Methods* **1983**, *65*, 55–63.